Interfacial Shear Strength (IFSS) and Absorbed Energy Versus Temperature in Carbon Fiber-Thermoplastic Composites via Single Fiber Pullout Testing

BRANNDON R. CHEN[1,2,*], NITHIN K. PARAMBIL[1], JOSEPH M. DEITZEL[1], JOHN W. GILLESPIE JR.[1,2,3,4,5], LOAN T. VO[6] and PETER SAROSI[6]

ABSTRACT

Single-fiber micromechanical experiments are often conducted to obtain interface properties between the matrix and fiber in fiber reinforced composites. This study investigates the apparent interfacial shear strength in AS4/polypropylene composites using the single fiber pullout test at sub-ambient, ambient, and elevated temperatures. Fiber failure surfaces are examined (using scanning electron microscopy) to identify the failure mechanisms present and embedded length of the fiber. The results indicate a higher IFSS at low temperatures than at elevated temperatures. Specific energies associated with debonding frictional sliding are also shown to be inversely temperature dependent. The failure mode transitions from cohesive failure in the matrix at room temperature and elevated temperatures to interfacial failure at the lowest temperature. This experimental setup and results will help to understand the temperature dependent failure mechanisms in polymer composite systems across a range of temperatures.

[1]Center for Composite Materials, University of Delaware. Newark, DE 19716, USA
[2]Department of Materials Science and Engineering, University of Delaware. Newark, DE 19716, USA
[3]Department of Mechanical Engineering, University of Delaware. Newark, DE 19716, USA
[4]Department of Civil and Environmental Engineering, University of Delaware. Newark, DE 19716, USA
[5]Department of Computer and Electrical Engineering, University of Delaware. Newark, DE 19716, USA
[6]ExxonMobil Research and Engineering Company, Annandale, NJ 08801, USA

INTRODUCTION

Thermoplastic olefins are a commodity class of material commonly used in consumer goods. The low cost of and known history of processing resins make them attractive for commercial mass production. However, this class of material suffers from creep-rupture failure because of the viscoelastic behavior when operating at .. om temperature, which is above the materials' T_g[1]. Fiber reinforcing the matrix is a solution to mitigate the creep-rupture response and increase the overall performance.

In fiber reinforced composite systems there are four main energy absorbing mechanisms: fiber breakage; resin plasticity; interface debonding between the fiber and matrix; and frictional sliding between the debonded fiber and matrix. All except for fiber breakage, in polymer systems are influenced directly by the viscoelastic response of the matrix. These composite material systems must be able to perform over a wide operating temperature range, typically for polypropylene -40°C to 126°C[2]. Temperature, stress, and strain-rate are three major factors that influence the viscoelastic response of the matrix and thus the composite performance. It has been shown that micro-mechanical performance correlates to macro-scale composite properties[3].

Historically IFSS studies manipulated interface strength by the application of a fiber sizing and surface treatments[3–5]. In this study we manipulate the interfacial shear strength (IFSS) and thus energy absorption by changing the yield stress of the matrix, which for polypropylene is highly temperature dependent[6]. Frictional sliding is influenced by the CTE shrinkage and crystallization of the resin that produces radial compression around the fibers. Lower temperature will have higher clamping pressure on the fiber, therefore have a higher friction force. The temperature dependent viscoelastic properties of the polypropylene leading to stress relaxation directly competes with the radial compression and frictional forces. In this study we hold strain rate and crystallinity constant while varying temperature to understand the effects on IFSS and energy absorption.

Micromechanical testing is employed to quantify the interfacial shear strength and gage the composite material system's performance. For polypropylene (PP) we can easily test below and above the glass transition temperature. The pullout test method has the advantage over other methods, such as single fiber fragmentation, because the fiber failure surface can be observed to identify failure mechanisms present. These experimental results and test setup lay the groundwork for developing a complete FE/Experimental model that will help better understand failure modes across a range of temperatures a fiber polymer matrix composite may experience.

Experimental

SAMPLE PREPARATION

Fiber pullout specimens were fabricated using ExxonMobil PP3155 polypropylene blended with 10% ExxonMobil PO1024 MAPP adhesion promoter. The bulk crystallinity of the pullout samples was found to be 62% using a NETZSCH DSC214 Polyma (Netzsch, GmbH). The glass transition temperature was found to be 3°C using a Mettler-Toledo DMA (Mettler-Toledo, LLC).

Unsized Hexcel AS4 carbon fibers were used in this study. A FIMABOND (TexTechno, GmbH.) was used for pullout sample preparation. Polypropylene disks of 5mm diameter were punched from sheets and placed on aluminum sample stubs (crucibles). These stubs were modified, by milling and grit blasting, from the original design to mitigate air bubble formation when using disks of the polymer feedstock. Single fibers were then inserted a nominal 100µm (at 100µm/min) into the molten matrix once the temperature stabilized at 220°C. The pullout specimens were then force air cooled to room temperature. Figure 1 shows a schematic of the fiber pullout specimen.

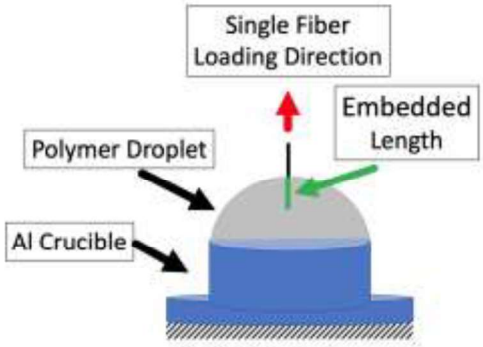

Figure 1. Schematic of a fiber pullout specimen.

The pullout tests were performed in a modified Instron 5848 MicroTester (Instron Corp.) Modifications are described in detail in the next sub-section. After testing and sample failure, fiber embedded length was measured via scanning electron microscope.

INSTRON 5848 LOAD SETUP

An Instron 5848 MicroTester equipped with a temperature chamber was used for the test frame. A long sample mounting fixture was made to thread into a 2N load cell to prevent damage from the range of testing conditions. The load cell assembly was fitted to a X-Y stage for aligning the fiber to the fiber grips/loading direction. The fiber grips consisted of self-centering screw clamp mounted to the Instron crosshead. Urethane rubber was used to line the jaws in contact with the fiber to prevent damage and premature failure. A NIST calibrated thermocouple was used to verify the temperature conditions. Below in Figure 2 is an annotated picture of the load-frame test setup. For pullout testing, the crosshead displacement rate was 0.1mm/min.

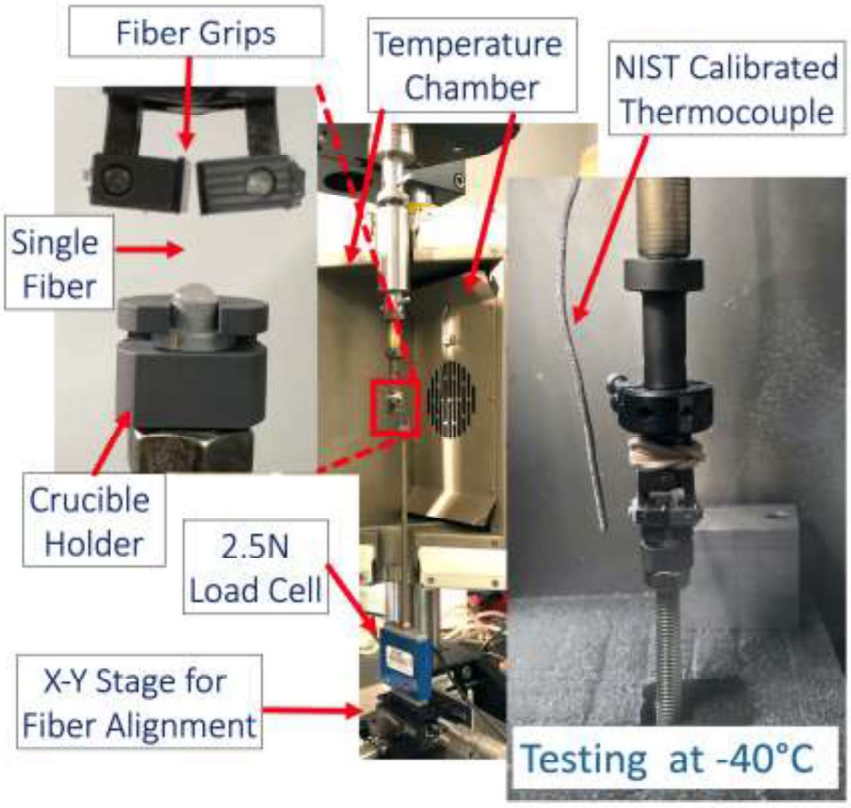

Figure 2. Test setup on the Instron 5848 MicroTester.

POLYPROPYLENE FILM TEST

Polypropylene film strips with a nominal gage dimension of 20 x 6 x 0.5mm were tested in an Instron 4484 (Instron Corp.) equipped with a temperature chamber and contactless video extensometer. Samples were tested from -40 to 75°C at a tensile strain rate of 1e-2 s^{-1}.

RESULTS AND DISCUSSION

POLYPROPYLENE YIELD STRESS VARIATION WITH TEMPERATURE

Yield stress was shown to decrease with increasing temperature in Figure 3. All yield stress values had a standard deviation of ~0.3MPa or less. The temperature dependent yield stress is an important factor given that the matrix plasticity failure mechanism will begin around the fiber once this stress is reached in the matrix.

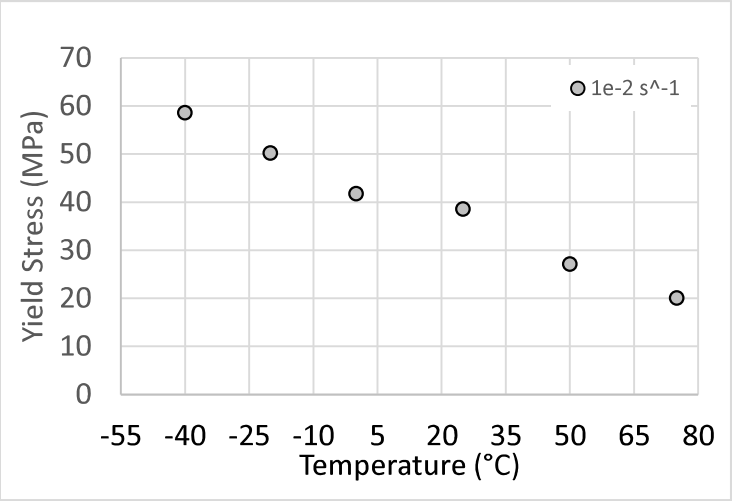

Figure 3. Polypropylene yield stress vs temperature.

INTERFACIAL SHEAR STRENGTH AND MECHANISMS VS TEMPERATURE

Interfacial shear strength measurements had a clear relation to the testing temperature conditions. All specimens failed in a uniform manner with embedded lengths averaging 85 ± 10μm (SEM measurements). Below in Figure 4 are representative force-displacement curves for each of the three different temperatures tested. The IFSS is calculated from the following formula:

$$IFSS = \frac{Peak\ Load}{Embedded\ Surface\ Area} \quad (1)$$

Embedded surface area was calculated from SEM imaging measurements on each fiber failure surface. Specimens were disregarded when the corresponding fiber failure surface could not be retrieved/imaged.

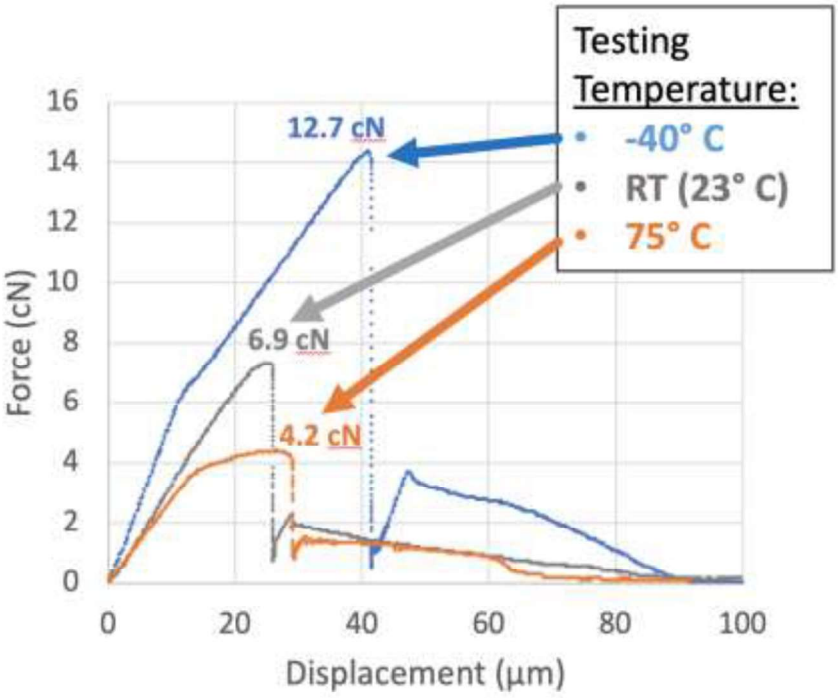

Figure 4. Force-Displacement curves for three tests conditions; -40°C, 23°C, and 75°C.

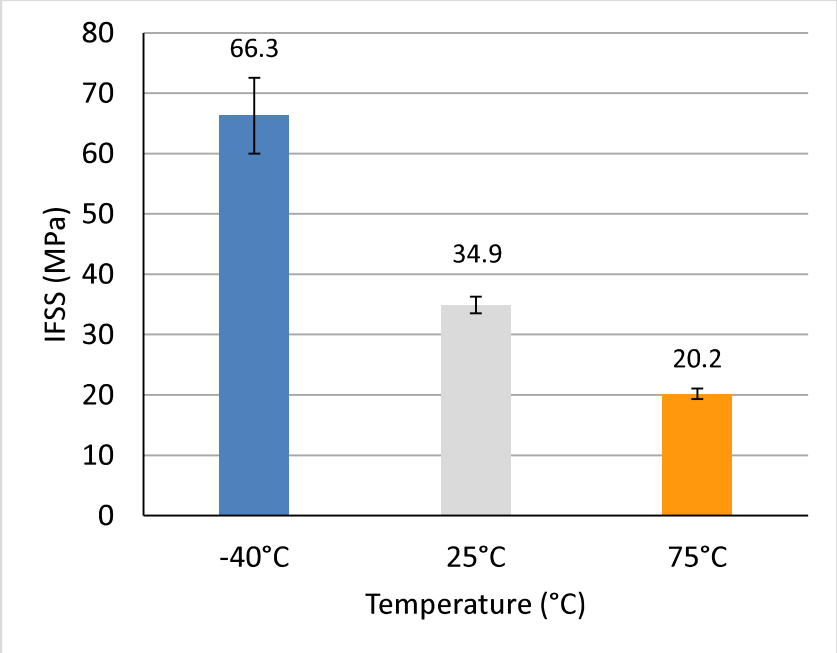

Figure 5. Apparent IFSS versus testing temperature.

Figure 5 shows the summarized IFSS results for the three temperature conditions. Tests conducted at -40°C had the highest IFSS of 66.3 MPa. The coefficient of variation (CV) is highest for the lowest temperature (-40°C, 14%), where adhesive failure is observed, and decreases as testing temperature increase and

shifts to cohesive failure (23°C, 13%; 75°C, 4%). It is worth noting that this value is twice the IFSS for room temperature, and the value is within the range of a high-performance thermoplastic fiber composite. Such high IFSS can be attributed to several temperature dependent factors such as, increased yield strength at below T_g, increased residual radial and CTE/clamping force, and the covalent bonding between the fiber and the maleic anhydride graft polypropylene (MAPP) additive in the polypropylene. At temperatures above the T_g, at room temperature and above at 75°C, IFSS was 34.9 and 20.2 MPa, respectively. At these higher temperatures, the residual force after failure (representing frictional sliding) indicates less radial clamping around the fiber. These can be explained by less CTE shrinkage. At the 75°C test temperature, there is a step feature in the frictional sliding region compared to the other two cases which are linearly decreasing. PP bonded to the fiber could provide additional surface roughness leading to the higher sliding force.

The force-displacement curves, shown in Figure 4, highlight important clues to the mechanisms leading up to and at failure of the specimen. The curves for the test conducted at -40°C were linear up to peak load with a sharp drop upon failure. When testing above T_g, both at 23°C and 75°C, there is no sharp peak but instead, a rounded drawn-out peak. Matrix yielding is the most likely explanation for the blunt peak around maximum load. Aside from the lower IFSS, the peak was extended further at the highest temperature, an indication more yielding is occurring. This trend is further supported by the temperature dependent yield stress shown earlier. MAPP additives have been shown to chemically react with amine and hydroxyl functional groups[7–9]. On unsized carbon fibers, these functional groups are still present from production process[10]. The residual matrix sheath around the specimens at 23°C and 75°C suggests the covalent bonding is sufficiently stronger, however the matrix yielding dominates as the molecular entanglements holding the PP and MAPP chains together are weaker than the covalent bonds between the MAPP and fiber.

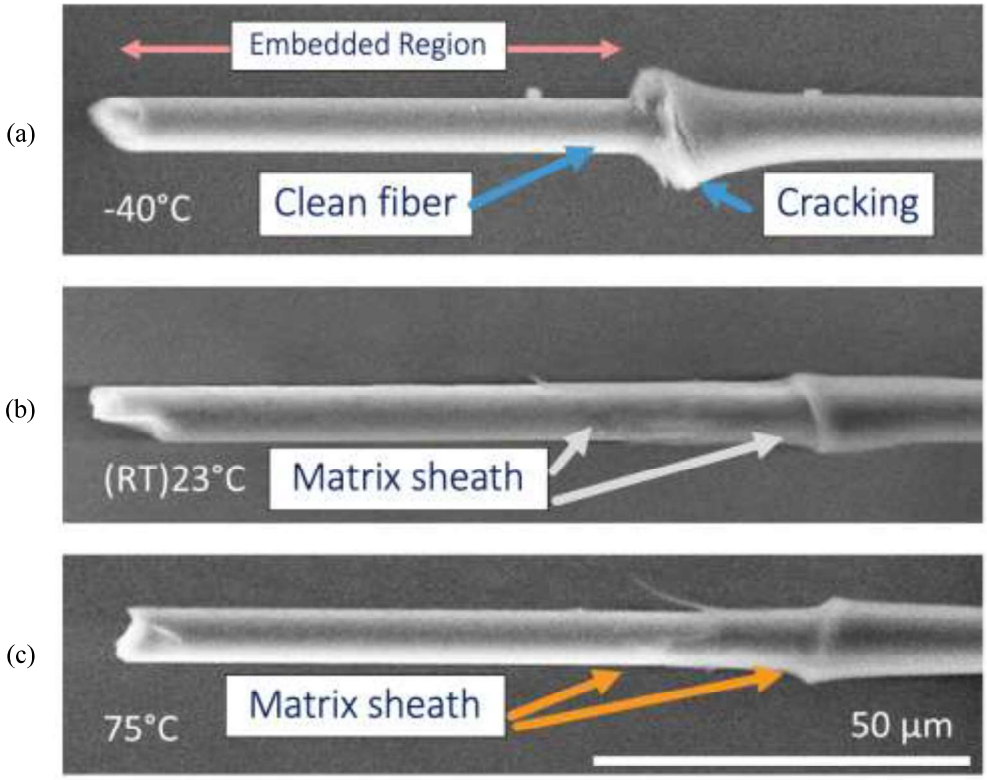

Figure 6. SEM micrographs of (a) -40°C, (b) 23°C, and (c) 75°C.

The SEM images of the three different temperatures in Figure 6 indicate different failure modes and can be correlated to their respective force displacement curve. The SEM image in Figure 6a shows a fiber failure surface after testing a -40°C. At the resin cap there are cracks present and a clean fiber surface below. The corresponding load-displacement curve exhibits a sudden drop in load, this would be attributed to brittle failure and/or debonding (adhesive failure), where little yielding would be expected. At the elevated testing temperatures, both 23°C and 75°C (Figure 6b and Figure 6c, respectively), there is a residual matrix sheath below the resin cap, running 10-30µm. The 75°C test conditions exhibited long strands of PP stretched away from the fiber. This provides a clear indication of matrix plasticity or yield occurring at failure.

ENERGY ABSORPTION VS TEMPERATURE

Recall the 4 mechanisms of composite failure, two of these mechanisms can be quantified from the force-displacement curve seen in Figure 4. Energy absorption from the pullout test can be defined in two parts: the debonding energy, associated with the initial loading region of the force-displacement; and the frictional sliding energy. Gao used a similar methodology to compare the energy absorption between glass fibers with different surface treatments using the microdroplet test[11]. The specific debonding energy, per embedded area, can be used directly since the embedded area does not change during loading. However, to adapt the specific energy for sliding, the integral must include the reduction in area as a function of displacement. Equation 2 defines the specific energy as the area under the force (F) vs displacement (x) curve per embedded area:

$$E^{Specific} = \int_{x_1}^{x_2} \frac{F(x)}{A(x)}\, dx \qquad (2)$$

This is valid for both debonding and frictional sliding. For the debonding case, A(x) is constant as the embedded length remains the same through the initial loading region (x_1=0, and x_2 = position of peak load). For frictional sliding, the embedded length/area, A(x), changes between x_1, at the beginning of sliding, and x_2, when the fiber has completely pulled out.

The specific energy associated with debonding versus temperature can be seen in Figure 7. At -40°C, the specific energy is 3 times higher than 23°C and almost 5 times higher than 75°C. The specific energy is 2 times higher at 23°C than at 75°C. Recall the matrix yield stress decreases with increasing temperature. The debonding energy reflects how much load is stored in the interface region, as a result of covalent interface bonding, radial clamping force, and matrix yield stress. As the temperature increases, the yield stress decreases and therefore less energy can be stored in this region before catastrophic failure occurs. In the case of the -40°C conditions, the SEM micrograph shows a clean fiber surface with no residual matrix sheath and cracking at the meniscus. This is an indication the energy associated with debonding was less than that to yield, causing interfacial debonding to be the dominant mechanism. At the elevated temperatures, the long strands of residual matrix on the fibers indicate matrix yielding as the dominant mechanism.

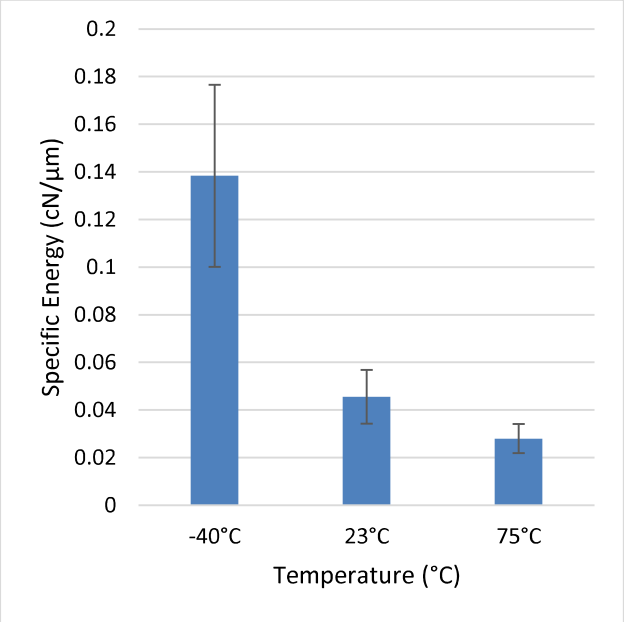

Figure 7. Specific energy associated with debonding.

The specific energy associated with frictional sliding versus temperature can be seen in Figure 8. The lowest temperature has the highest specific energy, about twice as much as both elevated temperature tests. This is consistent as the frictional sliding energy is directly related to the radial clamping pressure of the debonded matrix on the fiber. The frictional force is related to the CTE stresses, which are influenced by the testing temperature conditions, but also to the residual rubble that is still bonded to the debonded fiber.

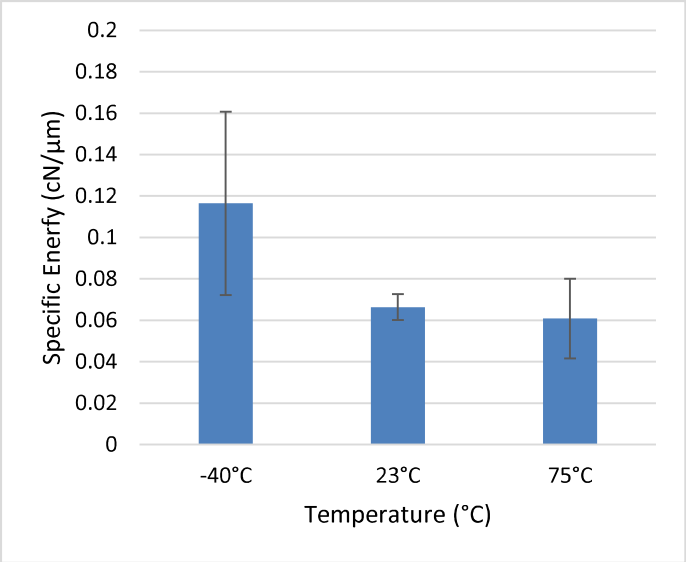

Figure 8. Specific energy associated with frictional sliding.

CONCLUSION

Fiber pullout IFSS, energy absorption mechanisms and corresponding failure modes show a strong inverse temperature dependence. The failure mode transitions from adhesive interfacial failure at low temperature to cohesive matrix failure at room temperature and above. SEM imaging provided evidence of the brittle to ductile failure mechanism change as temperature increased. The IFSS, specific debonding energy, and frictional sliding energy absorption decreased with increasing test temperature and can be explained by the inverse temperature dependence of the matrix yield stress. This experimental work lays the groundwork for understanding the complex interactions and failure mechanisms between the fiber/interface/matrix across a composite's service temperature range.

FUTURE WORK

We hypothesize that there is a crucial temperature and strain-rate window near the polymers T_g at which the failure mode will transition from adhesive to cohesive. Furthermore, we believe that this trend would be universal to other polymer-fiber systems tested below, at, and above the materials' glass transition. A corresponding FE pullout model is being developed to isolate the mechanisms seen in these experiments. This will be used to generate traction separation laws that will serves as inputs to micro/macro-scale composite models to study the temperature dependent viscoelastic response of short fiber composites.

ACKNOWLEDGEMENTS

This research was sponsored by ExxonMobil Research and Engineering Company.

REFERENCES

[1] Dixon-Stubbs PJ. Creep behaviour of: polyethylene and polypropylene. vol. 16. 1981.

[2] Richardson TL, Lokensgard E. Industrial Plastics: Theory and Applications. Thomson Delmar Learning; 2004.

[3] Mäder E, Grundke K, Jacobasch HJ, Wachinger G. Surface, interphase and composite property relations in fibre-reinforced polymers. Composites 1994;25:739–44. https://doi.org/10.1016/0010-4361(94)90209-7.

[4] Mäder E, Jacobasch HJ, Grundke K, Gietzelt T. Influence of an optimized interphase on the properties of polypropylene/glass fibre composites. Compos Part A Appl Sci Manuf 1996;27:907–12. https://doi.org/10.1016/1359-835X(96)00044-9.

[5] Yang L, Thomason JL. Interface strength in glass fibre–polypropylene measured using the fibre pull-out and microbond methods. Compos Part A Appl Sci Manuf 2010;41:1077–83. https://doi.org/10.1016/J.COMPOSITESA.2009.10.005.

[6] Hartmann B, Lee GF, Wong W. Tensile yield in polypropylene. Polym Eng Sci 1987;27:823–8. https://doi.org/10.1002/pen.760271109.

[7] Nygård P, Redford K, Gustafson C-G, Gustafson C. Composite Interfaces Interfacial strength in glass fibre-polypropylene composites: influence of chemical bonding and physical entanglement Interfacial strength in glass bre-polypropylene composites: inn uence of chemical bonding and physical entanglement. Compos Interfaces 2002;9:365–88. https://doi.org/10.1163/156855402760194719.

[8] Mutjé P, Vallejos ME, Gironès J, Vilaseca F, López A, López JP, et al. Effect of maleated polypropylene as coupling agent for polypropylene composites reinforced with hemp strands. J Appl Polym Sci 2006;102:833–40. https://doi.org/10.1002/app.24315.

[9] Karsli NG, Aytac A. Effects of maleated polypropylene on the morphology, thermal and mechanical properties of short carbon fiber reinforced polypropylene composites. Mater Des 2011;32:4069–73. https://doi.org/10.1016/j.matdes.2011.03.021.

[10] Dilsiz N, Wightman JP. Surface analysis of unsized and sized carbon fibers. Carbon N Y 1999;37:1105–14. https://doi.org/10.1016/S0008-6223(98)00300-5.

[11] Gao X, Jensen RE, Li W, Deitzel J, McKnight SH, Gillespie JW. Effect of Fiber Surface Texture Created from Silane Blends on the Strength and Energy Absorption of the Glass Fiber/Epoxy Interphase. J Compos Mater 2008;42:513–34. https://doi.org/10.1177/0021998307086203.